

## REFERENCES AND NOTES

- H. Finkelmann, M. Happ, M. Portugall, H. Ringsdorf, *Makromol. Chem.* **179**, 2541 (1978).
- H. Finkelmann, H. Ringsdorf, W. Siol, J. H. Wendorff, in *Mesomorphic Order in Polymers and Polymerization in Liquid Crystal Media*, A. Blumstein, Ed. (American Chemical Society, Washington, DC, 1978).
- R. B. Meyer, L. Liebert, L. Strzelecki, P. Keller, *Mol. Cryst. Liq. Cryst.* **38**, L-69 (1975).
- N. A. Clark and S. T. Lagerwall, *Appl. Phys. Lett.* **36**, 899 (1980).
- J. C. Jones, M. J. Towler, J. R. Hughes, *Displays* **14**, 86 (1993).
- V. Shibaev, M. Kozlovsky, L. Beresnev, L. Blinov, A. Platé, *Polym. Bull.* **12**, 299 (1984).
- S. Uchida, K. Morita, K. Miyoshi, K. Hashimoto, K. Kawasaki, *Mol. Cryst. Liq. Cryst.* **155**, 93 (1988).
- H. Kelker, R. Hatz, C. Schumann, *Handbook of Liquid Crystals* (Verlag Chemie, Weinheim, Germany, 1980), p. 111.
- B. P. Griffin and M. K. Cox, *Br. Polym. J.* **12**, 147 (1980).
- A. N. Semenov, *Mol. Cryst. Liq. Cryst.* **209**, 191 (1991).
- M. V. Kozlovsky, L. Bata, K. Fodor-Csorba, V. P. Shibaev, *Cryst. Res. Technol.* **27**, 1141 (1992).
- S. Hanna, A. Romo-Uribe, A. H. Windle, *Nature* **366**, 546 (1993).
- H. Finkelmann, H. J. Koch, G. Rehage, *Makromol. Chem. Rapid Commun.* **2**, 317 (1981).
- N. R. Barnes, F. J. Davis, G. R. Mitchell, *Mol. Cryst. Liq. Cryst.* **168**, 13 (1989).
- C. Degert, H. Richard, M. Mauzac, *ibid.* **214**, 179 (1992).
- C. Degert, P. Davidson, S. Megtert, D. Petermann, M. Mauzac, *Liq. Crystals* **12** (no. 5), 779 (1992).
- R. A. M. Hikmet and J. A. Higgins, *ibid.*, p. 831.
- A. J. Symons, F. J. Davis, G. R. Mitchell, *ibid.* **14** (no. 3), 853 (1993).
- F. H. Kreuzer, *Proc. 11. Freiburger Arbeitstagung Flüssigkristalle* (University of Freiburg, Freiburg, Germany, 1981), p. 5.
- \_\_\_\_\_, M. Gawhary, R. Winkler, H. Finkelmann, European Patent EP0060335 (1981).
- R. D. C. Richards *et al.*, *J. Chem. Soc. Chem. Commun.* **1990**, 95 (1990).
- F. H. Kreuzer *et al.*, *Mol. Cryst. Liq. Cryst.* **199**, 345 (1991).
- B. Reck and H. Ringsdorf, *Makromol. Chem. Rapid Commun.* **6**, 291 (1985).
- Idemitsu Display demonstrated at Fourth International Conference on Ferroelectric Liquid Crystals, 28 September to 1 October 1993, Tokyo, Japan.
- K. Yuasa *et al.*, U.S. Patent 5,069,533 (1991).
- R. G. Keppeler and R. A. Anderson, *J. Appl. Phys.* **49**, 4490 (1978).
- L. M. Blinov, L. A. Beresnev, N. M. Shtykov, Z. M. Elashvili, *J. Phys. (Paris)* **40** (no. 4), C3 (1979).
- L. A. Beresnev and L. M. Blinov, *Ferroelectrics* **33**, 129 (1981).
- A. Kokot, R. Wrzallik, J. K. Vij, R. Zentel, *J. Appl. Phys.* **75**, 728 (1994).
- J. W. O'Sullivan, Y. P. Panarin, J. K. Vij, *ibid.* **77**, 1201 (1995).
- This article is published with the permission of the Controller of Her Britannic Majesty's Stationery Office.

# Structure in Thin and Ultrathin Spin-Cast Polymer Films

C. W. Frank, V. Rao,\* M. M. Despotopoulou,† R. F. W. Pease, W. D. Hinsberg, R. D. Miller, J. F. Rabolt‡

The molecular organization in ultrathin polymer films (thicknesses less than 1000 angstroms) and thin polymer films (thicknesses between 1000 and 10,000 angstroms) may differ substantially from that of bulk polymers, which can lead to important differences in resulting thermophysical properties. Such constrained geometry films have been fabricated from amorphous poly(3-methyl-4-hydroxy styrene) (PMHS) and semicrystalline poly(di-*n*-hexyl silane) (PD6S) by means of spin-casting. The residual solvent content is substantially greater in ultrathin PMHS films, which suggests a higher glass transition temperature that results from a stronger hydrogen-bonded network as compared with that in thicker films. Crystallization of PD6S is substantially hindered in ultrathin films, in which a critical thickness of 150 angstroms is needed for crystalline morphology to exist and in which the rate of crystallization is initially slow but increases rapidly as the film approaches 500 angstroms in thickness.

A synthetic polymer exhibits substantial interdependence among its chemical composition, processing protocol, and morphological structure and among its resulting mechanical, thermal, optical, and electrical properties. Typically, the bulk physical parameters depend on the macromolecular nature of the material, with the character-

istic molecular dimension being the radius of gyration  $R_g$ , which is proportional to the square root of the molecular weight. For typical commercial polymers having molecular sizes in the range of 100,000 daltons,  $R_g$  might be on the order of 100 Å. In the bulk state, a particular "test chain" such as might be isolated through selective deuteration and measured by neutron scattering, exhibits a Gaussian distribution of the distances of one chain end from the other. About 1% of the volume within the roughly spherical domain encompassing this test chain is occupied by the chain itself, with the remainder being occupied by many other intertangled chains. This picture of the amorphous solid state, first predicted by P. J. Flory in 1953 and subsequently verified by neutron scattering, is well accepted for the bulk state. However, relatively recent simulations indicate that the picture must be

modified for regions near solid substrates and for polymer films of constrained geometry, such as those whose film thickness is comparable to a small multiple of  $R_g$  (1).

Such constrained geometry films may be classified as "ultrathin" for thicknesses <1000 Å and as "thin" for thicknesses between 1000 and 10,000 Å (1 μm). Ten Brinke (2) performed lattice Monte Carlo (MC) simulations on a polymer melt confined between parallel plates and found variations in chain conformation when the distance between the plates was comparable to  $2R_g$ . In off-lattice MC simulations, Kumar (3) found two correlation length scales: Single-chain properties were disturbed over a distance comparable to  $2R_g$ , whereas many chain properties were screened out at a length three times the monomer segment size. Molecular dynamics simulations of confined chains showed that the solid-melt interface is approximately two segment diameters thick and the segment mobility is highly anisotropic in the interfacial region (4). Finally, self-consistent field lattice model calculations (5) of polypropylene on graphite showed an enrichment of the interface with polymer ends, some flattening of the chains parallel to the substrate, and anisotropic molecular mobilities.

## Application Issues for Polymer Thin Films

Although mechanical applications of polymers take advantage of their bulk properties, there are numerous technologies in which ultrathin and thin polymer films are found. For example, they are used as resists and interlayer dielectrics in microelectronics fabrication, as alignment layers in liquid crystal displays, and as lubricants in magnetic information storage devices. In each of these applications, the polymer chain orientation and state of organization play important

C. W. Frank, V. Rao, and M. M. Despotopoulou are in the Department of Chemical Engineering, Stanford University, Stanford, CA 94305-5025, USA. R. F. W. Pease is in the Department of Electrical Engineering, Stanford University, Stanford, CA 94305, USA. W. D. Hinsberg, R. D. Miller, and J. F. Rabolt are at the IBM Almaden Research Center, IBM Research Division, 650 Harry Road, San Jose, CA 95120-6099, USA.

\*Present address: Intel Corporation, 2200 Mission College Boulevard, Santa Clara, CA 95052, USA.

†Present address: Elf Atochem N.A., 900 First Avenue, Post Office Box 61536, King of Prussia, PA 19406, USA.

‡Present address: University of Delaware, Materials Science Program, Spencer Laboratory, Newark, DE 19716, USA.

roles in determining the final properties.

1) Although the polymer resist is not present in the final microprocessor chip, it is used many times in patterning the circuitry. The need to minimize pinhole defects requires that the polymer resist films in current technology be in the range of 0.4 to 1.0  $\mu\text{m}$  thick. If such defects can be eliminated for much thinner films, perhaps through understanding of de-wetting phenomena, circuits of potentially higher density might be patterned.

2) In the interlayer dielectric application, polymer thin films exhibit lower dielectric constants than do inorganic glasses for separation of lines of metallization and thus could potentially provide faster circuitry with less cross-talk. However, there are often severe problems with mismatch in the coefficients of thermal expansion that can cause delamination of the polymer from the metal or from a ceramic substrate. Reduction of this mismatch requires understanding of the relation between the molecular composition of the polymer and the processing protocol that was used to deposit the film.

3) Virtually all liquid crystal displays, such as those found in digital watches, have a polymer film alignment layer that is used to promote specific in-plane and out-of-plane orientation of liquid crystalline molecules of low molecular weight that are placed in contact with the film. Although such surface-induced orientation is essential to the operation of the display, the mechanical rubbing process that is used to produce the alignment layer and the relative importance of surface chemistry and topography are poorly understood.

4) The hard disk of the desktop personal computer must be able to go from being stationary to high rates of revolution without causing any damage to either the magnetic read/write head or the magnetic media on the disk. Both the static friction associated with start-up and the dynamic friction associated with steady operation are reduced by lubricants, which include a variety of polymeric materials. An understanding of the dynamic response of the attached polymer chains is necessary in order to optimize disk performance.

### Spin-Casting

The films described above are usually fabricated by spin-casting, which is done by placing a small quantity of polymer solution on a flat substrate and then rotating the substrate at a particular angular rate for a specified time. The resulting film is usually annealed to remove residual solvent and to relax internal stresses. This process is conceptually simple, but the interplay of polymer molecular structure and processing protocol is actually complex, particularly when

the film thickness drops substantially into the submicrometer regime. In the most comprehensive treatment of the rheology of spin-casting to date, Bornside *et al.* (6) divided spin-casting into deposition, spin-up, spin-off, and solvent evaporation. During the first three stages, film thickness is dictated by the centrifugal forces, but during the final stage, the increasing viscosity of the solution, the rate of solvent evaporation, and shear thinning of the fluid all must be taken into consideration.

Although the majority of spin-casting studies have been directed toward predicting final film thickness and uniformity, relatively little attention has been paid to structure at the molecular level. Some guidance has been given by early work on static-cast films. Croll (7) found that substantial in-plane stresses were set up in the film that were due to shrinkage during solvent evaporation. Prest and Luca (8) found that the birefringence of 1- to 5- $\mu\text{m}$ , static-cast polystyrene and polycarbonate films increased as the film thickness decreased, indicating a higher in-plane orientation in the thinner films. Cohen and Reich (9) found that polymers of high molecular weight exhibited long-range order, up to 10  $\mu\text{m}$  from the substrate, whereas films containing materials of low molecular weight were only ordered over the first micrometer. Residual stresses have been the focus of studies on spin-cast polyimide precursors by Ree *et al.* (10), in which the stress was attributed primarily to a mismatch of thermal coefficients of expansion, which in turn may be related to chain conformation. Recent studies (11–13) have shown that the strength of adhesion between the polymer and the substrate substantially affects both the thermal expansion coefficient and the glass transition temperature ( $T_g$ ) in ultrathin polymer films.

The objective of this general article is to explore the effect of film thickness on polymer organization in thin and ultrathin films. Spin-casting has been selected as the fabrication technique because of its widespread technological use, but other methods are being studied in our laboratories, including the formation of Langmuir-Blodgett multilayers, alternating polycation-polyanion deposition, and a variety of surface-grafting methods. The latter permit study of how strong surface interactions (such as covalent bonding) influence thermophysical properties and provide a counterpoint to the physisorbed systems, such as those obtained for spin-casting. Specifically, we discuss the amount of residual solvent and the variation in hydrogen bonding and their effect on  $T_g$  in thin films of poly(3-methyl-4-hydroxy styrene) (PMHS) (14) as well as the morphology and kinetics of crystallization in ultrathin films of poly(di-n-hexyl

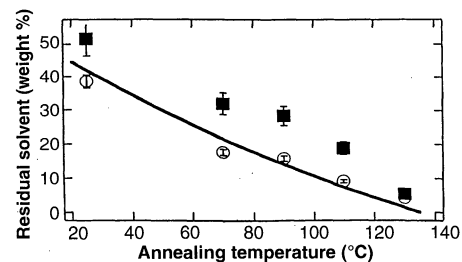


**Fig. 1.** Annealing temperature dependence of residual propylene glycol methyl ether solvent in 0.11- $\mu\text{m}$  (circles) and 1.2- $\mu\text{m}$  (squares) PMHS spin-cast films annealed for 1300 min. The solid line is the Flory-Fox prediction of the dependence of  $T_g$  on the residual solvent content; there are no adjustable parameters.

silane) (PD6S) (15). Both materials have links to current microlithographic technology in that PMHS is used as an inert matrix resin in deep ultraviolet (UV) resists, whereas PD6S has been explored as a UV resist that is capable of self-development. Although we discuss only these two specific applications, we believe that the behavior of these materials in ultrathin films is representative of strongly interacting amorphous polymers and semicrystalline polymers, respectively. Moreover, these results should also reflect morphological features of much thicker materials in the region immediately adjacent to a solid substrate.

### Structure in Ultrathin Polymer Films

*Residual solvent in thin films of PMHS.* The presence of residual solvent in spin-cast films is not unanticipated, but study of its consequences has been mainly restricted to its influence on the film dissolution rate, primarily because of its relevance to microlithographic processing. Schlegel (16) has explored multicomponent films, as are used in most photoresists, and related increased additive mobility to higher residual solvent levels. In addition, Beuchemin (17) has observed surface depletion of solvent during annealing below  $T_g$ , whereas uniform solvent distribution was found above  $T_g$ . In the present study, we focus on sub- $T_g$  annealing, which is typically practiced in microelectronics fabrication because of the thermal instability of the photoactive compounds in multicomponent photoresists. The important consequence is that we expect nonequilibrium structures induced during the spin-casting to remain in the films.

Figure 1 shows the residual solvent radiolabeling results of long-term steady-state (1300 min) annealing of 1.2- $\mu\text{m}$  and 0.11- $\mu\text{m}$  PMHS films at temperatures below the bulk  $T_g$  (135°C). Solvent retention is significantly greater in the 0.11- $\mu\text{m}$  films at all

temperatures except 130°C. Results for a 0.18- $\mu\text{m}$  film were similar to those for a 1.2- $\mu\text{m}$  film, which suggests a critical film thickness near 0.1  $\mu\text{m}$ . We assume that there are both mobile and bound solvent populations, with the mobile solvent being lost up to the point at which  $T_g$  approaches the annealing temperature and the bound solvent being retained by the polymer because of specific interactions, such as hydrogen bonding. To determine whether this bound solvent acts as a plasticizer capable of lowering  $T_g$ , we also plot in Fig. 1 the classic Fox equation (18), which is the simplest, zero-parameter model available for describing the reduction in  $T_g$  in polymers containing a low-molecular-weight solute. To apply this, we used the  $T_g$  of propylene glycol methyl ether acetate (PGMEA) of -56°C and observed good agreement with the 1.2- $\mu\text{m}$  film data, in spite of the simplicity of the model. The greater solvent content in the 0.11- $\mu\text{m}$  film is consistent with an effective  $T_g$  that is  $\approx 40^\circ\text{C}$  higher than for the thick film.

Further information about structural differences between the two films may be obtained from short-term transient annealing. A one-dimensional diffusion analysis (19) was performed that was based on the assumptions that the solvent diffusion coefficient is independent of concentration, that solvent concentration is initially uniform, and that there is an equilibrium, residual solvent concentration (the bound fraction). Diffusion coefficients determined by the fitting procedure are shown in Table 1. There is a dramatic difference, with the 0.11- $\mu\text{m}$  films having diffusion coefficients from 30 to 100 times smaller than those for the 1.2- $\mu\text{m}$  film. If we assume an Arrhenius-type temperature dependence, we see that this difference is largely due to the pre-exponential factors, which are  $5.2 \times 10^{-10}$  and  $2.0 \times 10^{-2}$   $\text{cm}^2/\text{s}$  for the thin and thick films, respectively. Corresponding activation energies are 1.61 and 4.06 kcal/mol.

It is likely that hydrogen bonding plays an important role in the PMHS-PGMEA films. In fact, Kwei *et al.* (20) and Painter *et al.* (21) have shown that polymer blends with strong hydrogen-bonding interactions can show a larger than expected  $T_g$ . To test this, we have used Fourier transform infrared spectroscopy (FTIR) to follow the O-H stretching frequencies, which are known (22) to reflect three situations: (i) free hydroxyls that do not participate in hydrogen bonds (shoulder at  $3536\text{ cm}^{-1}$ ), (ii) hydroxyl groups that are hydrogen-bonded with the solvent carbonyl group (broad band centered at  $3427\text{ cm}^{-1}$ ), and (iii) self-associated hydroxyl groups that engage in hydrogen bonding with other hydroxyl groups in the polymer (variable positions around  $3275\text{ cm}^{-1}$ ). The numbers in parentheses

are the band positions for the PMHS-PGMEA system. Whereas the first two types of O-H stretches were invariant with film thickness, annealing time, or temperature, the self-associated O-H bands were  $\approx 25\text{ cm}^{-1}$  lower for the 0.11- $\mu\text{m}$  films than for the 1.2- $\mu\text{m}$  film, indicating stronger hydrogen bonding in the thinner film. Moreover, the self-associated bands consistently shifted to lower energies with increasing annealing time or temperature; the maximum red shift of  $25\text{ cm}^{-1}$  was observed at  $110^\circ\text{C}$  for the thinner film.

*Crystallization of ultrathin films of poly(dihexyl silane).* Although the polymer modeling work described earlier makes unambiguous predictions about the changes in chain conformation near an interface, there have been few experimental tests. The polysilanes are ideally suited for such studies because their electronic properties depend strongly on the backbone conformation, which in turn influences the polymer morphology. Bulk PD6S films exhibit two intense UV absorption maxima, one at  $27,470\text{ cm}^{-1}$  and the other at  $31,650\text{ cm}^{-1}$  (23). FTIR and Raman spectroscopy; extended x-ray absorption fine structure, wide-angle x-ray, and electron diffraction; and  $^{13}\text{C}$  and  $^{29}\text{Si}$  solid state nuclear magnetic resonance studies show that the low-energy peak corresponds to an ordered crystalline phase, which occurs for temperatures below  $42^\circ\text{C}$ , whereas the high-energy peak corresponds to a disordered phase resulting at higher temperatures. The chain conformation in the ordered phase corresponds to long trans or nearly all-trans segments, whereas the Si backbone assumes a disordered helical conformation in the disordered phase (24). The film crystallinity may be estimated by spectral deconvolution, yielding values in agreement with x-ray diffraction and differential scanning calorimetry. Recently, Despotopoulou *et al.* (25) have shown that the degree of crystallinity depends strongly on the film thickness but is relatively independent of the surface chemical characteristics of the substrate. Figure 2 shows that crystallization is strongly hindered for ultrathin films, with crystal-

linity vanishing below about 150 Å.

Whereas electronic spectroscopy yields information on the PD6S backbone conformation, organization of the hexyl side chains of PD6S may be determined with FTIR. The most useful absorption bands are the  $1469\text{ cm}^{-1}$   $\text{CH}_2$  scissoring vibration and the  $2959\text{ cm}^{-1}$  asymmetric  $\text{CH}_3$  stretching vibration, with the former being highly sensitive to disorder and the latter, isotropic band being insensitive and thus useful for normalization. The 1469/2959 ratio decreased for film thicknesses  $< 2000\text{ Å}$ , ultimately vanishing at the same point at which the UV absorption results show totally amorphous structure. This result suggests that the disordering of the side chains (at  $2000\text{ Å}$ ) precedes the disordering of the backbone (at  $300\text{ Å}$ ). Combination of grazing incidence and transmission FTIR spectra leads to the conclusion that the backbone lies extended, with the polymer axis and extended hexyl side chains parallel to the plane of the film and with the hexyl carbon-carbon bond plane perpendicular to the substrate, but with some non-trans bonds present. This is consistent with work on spin-cast films (26) but is at variance with work on static-cast films (27) or films that have been subjected to extensive mechanical surface rubbing (28). Obviously, the type of processing plays an important role in the final polymer orientation and possibly in the morphology.

There have been several attempts to model the kinetics of polymer crystallization. One of the most widely used models is the Avrami-Evans theory (29). This simple theory treats crystallization as a macroscopic phenomenon in which nuclei appear at random points within the polymer volume and give rise to crystals that grow at a certain rate around the nuclei. Efforts to adapt this theory to thin polymer films have been made by Stein and Powers (30) and by Haudin and co-workers (31). We have examined the isothermal crystallization of films of PD6S that were spin cast, annealed at  $100^\circ\text{C}$  for 15

**Table 1.** Diffusion coefficients in square centimeters per second of propylene glycol methyl ether in PMHS films 0.11  $\mu\text{m}$  and 1.2  $\mu\text{m}$  thick, determined from a one-dimensional diffusion analysis of solvent loss during the first 2 hours of annealing at the temperatures indicated.

Temperature	0.11 $\mu\text{m}$ ( $\text{cm}^2/\text{s}$ )	1.2 $\mu\text{m}$ ( $\text{cm}^2/\text{s}$ )
$70^\circ\text{C}$	$4.2 \times 10^{-14}$	$1.2 \times 10^{-12}$
$90^\circ\text{C}$	$9.4 \times 10^{-14}$	$4.4 \times 10^{-12}$
$110^\circ\text{C}$	$1.1 \times 10^{-13}$	$1.4 \times 10^{-11}$

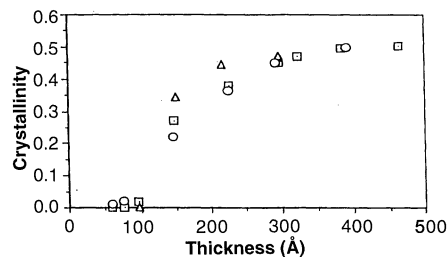


**Fig. 2.** Dependence of maximum attainable crystallinity, determined from UV absorption spectra, on thickness of PD6S films spin-cast on quartz (squares), hexamethyldisilazane-treated quartz (circles), or octadecyltrichlorosilane-treated quartz (triangles).

min, slowly cooled to 25°C and then cooled further to the desired crystallization temperature (32). Figure 3 shows the results of one series of kinetic experiments at a crystallization temperature of 0°C. The crystallization rate decreases dramatically as the film thickness decreases, particularly for thicknesses <300 Å. Moreover, over the range from 15° to -5°C, the rate of crystallization increased as the temperature decreased. The solid lines are the best fits of the Avrami equation to the experimental data. The fitting parameters for a film 500 Å thick vary with temperature, suggesting that the crystallization changes from a one-dimensional process to a three-dimensional process at a temperature between 5° and 0°C, possibly due to a transition from bulk to heterogeneous nucleation as the temperature increases.

## Discussion

Structure in ultrathin, spin-cast polymer films less than 1000 Å thick is substantially different from that in bulk materials. Although such heterogeneity is predicted by molecular modeling, experimental results from this study provide verification and further understanding. For example, the preferred chain alignment parallel to the solid substrate, which is expected from the modeling, may lead to the enhanced intermolecular hydrogen bonding observed in the amorphous PMHS. The substantial decrease in the residual solvent diffusion coefficient relative to that of the bulk state is consistent with this stronger network. One would expect the same phenomenon to apply during the reverse process of film dissolution; in fact, difficulties in removal of the

ultrathin "skin" are common in microelectronics processing.

PD6S adds a new level of complexity because of its ability to crystallize. If it is assumed that there is an aligned amorphous layer adjacent to the solid substrate, which is consistent with the modeling and PMHS results, we find it interesting that crystallization does not occur until thicknesses approach 150 Å. This critical thickness does not correspond to any intrinsic spatial dimension of the chain, such as cross-sectional thickness or  $R_g$ . However, it is precisely in the range of typical lamellar thicknesses for other semicrystalline polymers, which suggests that it may represent a critical nucleus thickness for surface-induced crystallization.

The results described herein for physisorbed, spin-cast, ultrathin polymer films represent one of the simpler manifestations of constrained geometry systems in which one of the physical dimensions of the material is comparable to a molecular dimension; in this case, the chain  $R_g$ . When the polymer chains are chemisorbed to the substrate, either through a "grafting to" approach in which a preformed polymer is bound to a chemically modified substrate or through a "grafting from" protocol involving surface-initiated polymerization, one expects to find a broader variety of chain conformations, such as in the form of extended brushes with controlled site density. These are also expected to exhibit interesting deviations of their thermophysical properties as compared with the bulk material.

## REFERENCES AND NOTES

- For a general review, see I. C. Sanchez, Ed., *Physics of Polymer Surfaces and Interfaces* (Butterworth-Heinemann, Boston, MA, 1992).
- G. ten Brinke, D. Auserre, G. Hadziioannou, *J. Chem. Phys.* **89**, 4374 (1988).
- S. K. Kumar, M. Vacatello, D. Y. Yoon, *ibid.*, p. 5206.
- I. Bitsanis and G. Hadziioannou, *ibid.* **92**, 3827 (1990).
- D. N. Theodorou, in (1), chap. 7.
- D. E. Bornside, C. W. Macosko, L. E. Scriven, *J. Imag. Tech.* **13**, 123 (1987).
- S. G. Croll, *J. Appl. Polym. Sci.* **23**, 847 (1979).
- W. M. Prest Jr. and D. J. Luca, *J. Appl. Phys.* **50**, 6067 (1979); *ibid.* **51**, 5170 (1980).
- Y. Cohen and S. Reich, *J. Polym. Sci. Polym. Phys.* **19**, 599 (1981).
- M. Ree, S. Swanson, W. Volksen, *Polymer* **34**, 1423 (1993).
- W. L. Wu, J. H. van Zanten, W. J. Orts, *Macromolecules* **28**, 771 (1995).
- W. E. Wallace, J. H. van Zanten, W. L. Wu, *Phys. Rev. E* **52**, R3329 (1995).
- J. H. van Zanten, W. E. Wallace, W. L. Wu, *ibid.* **53**, R2053 (1996).
- Two samples of PMHS were examined; the first was synthesized by means of the Heck reaction with weight-average molecular weight  $M_w$  of 12,400 and polydispersity  $M_w/M_n$  1.63; the second was a gift from M. T. Sheehan of Hoechst Celanese with  $M_w$  11,600 and polydispersity 2.1. For ellipsometry (Gaertner Scientific, Chicago, IL), transmission FTIR spectroscopy (Bio-Rad FTS 60A), and radiolabeling measurements, undoped silicon wafers 2.54 cm (1

inch) in diameter, polished on one side (Virginia Semiconductor, Fredericksburg, VA), were used after being cleaned (for 20 min in 70/21/9 volume %  $H_2SO_4/H_2O_2/H_2O$  followed by a rinse with distilled water). After spin-coating, films were annealed at 70°, 90°, 110°, or 130°C for up to 1300 min. PGMEA (Aldrich) was used as the spinning solvent. Radio-labeled PGMEA was prepared by reacting propylene glycol methyl ether with  $^{14}C$ -labeled acetyl chloride. Radioactivity measurements of residual, labeled PGMEA were made with a Packard Tri-Carb 460 liquid scintillation system.

- PD6S had  $M_w$   $2.6 \times 10^6$  with polydispersity of 2.4. For UV absorption (Varian Cary 3) and fluorescence (SPFX Fluorolog), quartz disks (Esco Products, Oak Ridge, NJ) were used after an etch procedure that was similar but included 30 s in buffered 1/6 HF/ $H_2O$  before the water rinse. Transmission FTIR (with an IBM IR 98) was done on KBr disks and silicon wafers, and reflection FTIR was done on glass slides having a 200 Å Cr adhesion layer overcoated with 2000 Å gold. Some quartz surfaces were treated with octadecyltrichlorosilane or hexamethyldisilazane to make them hydrophobic before PD6S deposition. Films were deposited by spin-casting from iso-octane solutions ranging from 0.1 to 2 weight % concentration at 3000 rpm for 40 s. Film thickness was determined with a Rudolph Research auto EL-II ellipsometer.
- L. Schlegel, T. Ueno, N. Hayashi, T. Iwayanagi, *J. Vac. Sci. Tech.* **B9**, 278 (1991).
- B. T. Beuchemin Jr., C. E. Ebersole, I. Daraktchiev, *SPIE* **2195**, 610 (1994).
- L. H. Sperling, *Introduction to Physical Polymer Science* (Wiley, New York, 1992), pp. 357-359.
- V. Rao, thesis, Stanford University (1994).
- T. K. Kwei, *J. Polym. Sci. Polym. Lett. Ed.* **22**, 307 (1984); T. Suzuki, E. M. Pearce, T. K. Kwei, *Polymer* **33**, 198 (1992); F. Wang, E. M. Pearce, T. K. Kwei, *J. Polym. Sci. Polym. Phys.* **29**, 619 (1991).
- P. C. Painter, S. L. Shenoy, D. E. Bhagwagar, J. Fishburn, M. M. Coleman, *Macromolecules* **24**, 5623 (1991).
- M. M. Coleman and P. C. Painter, *Appl. Spect. Rev.* **20**, 255 (1984); E. J. Moskala, D. F. Varnell, M. M. Coleman, *Polymer* **26**, 228 (1985); A. M. Lichkus, P. C. Painter, M. M. Coleman, *Macromolecules* **21**, 2636 (1988).
- R. D. Miller and J. Michl, *Chem. Rev.* **89**, 1359 (1989); R. D. Miller, D. Hofer, J. F. Rabolt, G. N. Fickes, *J. Am. Chem. Soc.* **107**, 2172 (1985); H. Kuzmany, J. F. Rabolt, B. L. Farmer, R. D. Miller, *J. Chem. Phys.* **85**, 7413 (1986).
- S. S. Patnaik and B. L. Farmer, *Polymer* **33**, 4443 (1992).
- M. M. Despotopoulou, R. D. Miller, J. F. Rabolt, C. W. Frank, *J. Polym. Sci. Polym. Phys. Ed.*, in press.
- R. D. Miller, R. Sooriyakumaran, J. F. Rabolt, *Bull. Am. Phys. Soc.* **32**, 886 (1987).
- F. C. Schilling, F. A. Bovey, A. J. Lovinger, J. M. Zeigler, in *Silicon-Based Polymer Science*, J. M. Zeigler, Ed. (ACS Symposium Series 224, American Chemical Society, Washington, DC, 1990), chap. 21.
- H. Tachibana, M. Matsumoto, Y. Tokura, *Macromolecules* **26**, 2520 (1993).
- M. Avrami, *J. Chem. Phys.* **7**, 1103 (1939); *ibid.* **8**, 212 (1940); *ibid.* **9**, 177 (1941); U. R. Evans, *Trans. Faraday Soc.* **41**, 365 (1945).
- R. S. Stein and J. Powers, *J. Polym. Sci.* **56**, 59 (1962).
- J. M. Escleine, B. Monasse, E. Wey, J. M. Haudin, *Colloid Polym. Sci.* **262**, 366 (1984); N. Billon, J. M. Escleine, J. M. Haudin, *ibid.* **267**, 668 (1989); N. Billon and J. M. Haudin, *ibid.*, p. 1064; N. Billon and J. M. Haudin, *Ann. Chim. Fr.* **15**, 249 (1990); N. Billon, C. Magnet, J. M. Haudin, D. Lefebvre, *Colloid Polym. Sci.* **272**, 633 (1994).
- M. M. Despotopoulou, C. W. Frank, R. D. Miller, J. F. Rabolt, *Macromolecules*, in press.
- Supported in part by the Polymers Program of ONR, the Sematech Center of Excellence on Lithography and Pattern Transfer, and the NSF-MRSEC Center on Polymer Interfaces and Macromolecular Assemblies (CPIMA).

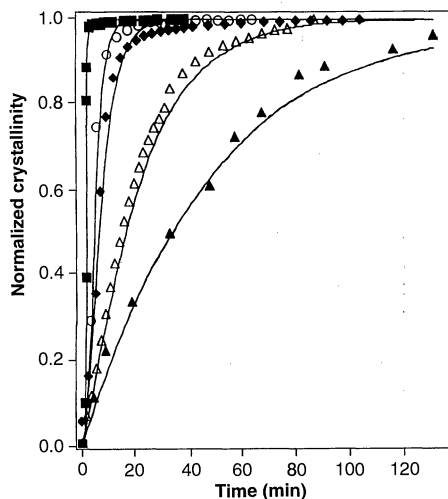


**Fig. 3.** Kinetics of crystallization at 0°C of spin-cast PD6S films of thickness 95 Å (solid triangles), 160 Å (open triangles), 220 Å (diamonds), 300 Å (circles), and 500 Å (squares). The solid lines are nonlinear fits of the Avrami equation to the normalized experimental crystallinity data.